



Dynamic Aperture for Single-Particle Motion: Overview of Theoretical Background, Numerical Predictions and Experimental Results

M. Giovannozzi

CERN AB/ABP

Summary:

- Definition
- Dynamic aperture computation
- Time-dependent effects
- Nonlinear dynamics experiments
- Dynamic aperture experiments:
FNAL - E778, DESY - HERA-p,
CERN - SPS
- Conclusions



Definition

A reasonable definition is the following

*Dynamic Aperture (DA) is the volume in phase space of the initial conditions that are stable for a given number **N** of turns in the accelerator.*

- ➡ From a physical point of view **N** is dictated by the specific problem, i.e. injection process duration, storage time etc.



DA computation 1/2

The DA computation can be performed by:

- ➡ **Direct computation:** the definition is applied, i.e. the evolution of a set of initial conditions is computed and the stable ones are kept for further analysis.
- ➡ This approach is very **CPU-time consuming**.
- ➡ It is affordable for **short- medium-term DA** computation, i.e. N not exceeding 10^4 - 10^5 (depending on the model).
- ➡ **Important remark: the computation can be parallelised!!!**



DA computation 2/2

- ➡ **Indirect computation:** the problem consists in looking for dynamics observables well-correlated with stability of initial conditions (**early indicators**).
- ➡ The computational effort should be **limited**.
- ➡ This approach is aimed particularly at **long-term** DA computation, i.e. N exceeding 10^6 .
- ➡ An example of a **semi-analytical** method for 2D maps will be given.



Direct DA computation 1/5

- ➡ According to the definition of DA in terms of volume in phase space, the following integral have to be computed:

$$\iiint \chi(x, p_x, y, p_y) dx dp_x dy dp_y$$

The function χ equals 1 if the initial condition (x, p_x, y, p_y) is stable for N turns.



Direct DA computation 2/5

If one neglects the **disconnected** part of the volume, then polar coordinates can be used

$$A_{\alpha, \vartheta_1, \vartheta_2} = \frac{1}{8} \int_0^{2\pi} \int_0^{2\pi} \int_0^{\pi/2} [r(\alpha, \vartheta_1, \vartheta_2)]^4 \sin(2\alpha) d\alpha d\vartheta_1 d\vartheta_2$$

DA as radius
of equivalent
hypersphere

$$r_{\alpha, \vartheta_1, \vartheta_2} = \left(\frac{2 A_{\alpha, \vartheta_1, \vartheta_2}}{\pi^2} \right)^{1/4}$$

Special weight!

In practice the integral is approximated by a sum...



Direct DA computation 3/5

$$r_{\alpha, \vartheta_1, \vartheta_2} = \left(\frac{\pi}{2KL^2} \sum_{k=1}^K \sum_{l_1=1}^L \sum_{l_2=1}^L \left[r(\alpha_k, \vartheta_{1l_1}, \vartheta_{2l_2}) \right]^4 \sin(2\alpha_k) \right)^{1/4}$$

- ➡ This approach allows determining the error due to the discretisation, i.e.
 - ➡ Discretisation in α -> error $\propto 1/K$
 - ➡ Discretisation in θ_1, θ_2 -> error $\propto 1/L$
 - ➡ Discretisation in r -> error $\propto 1/J$
- ➡ The step is optimised by imposing comparable errors on different variables. To have a relative error on DA of $1/(4J)$ -> J^4 , implying that $N \cdot J^4$ iterates are needed!



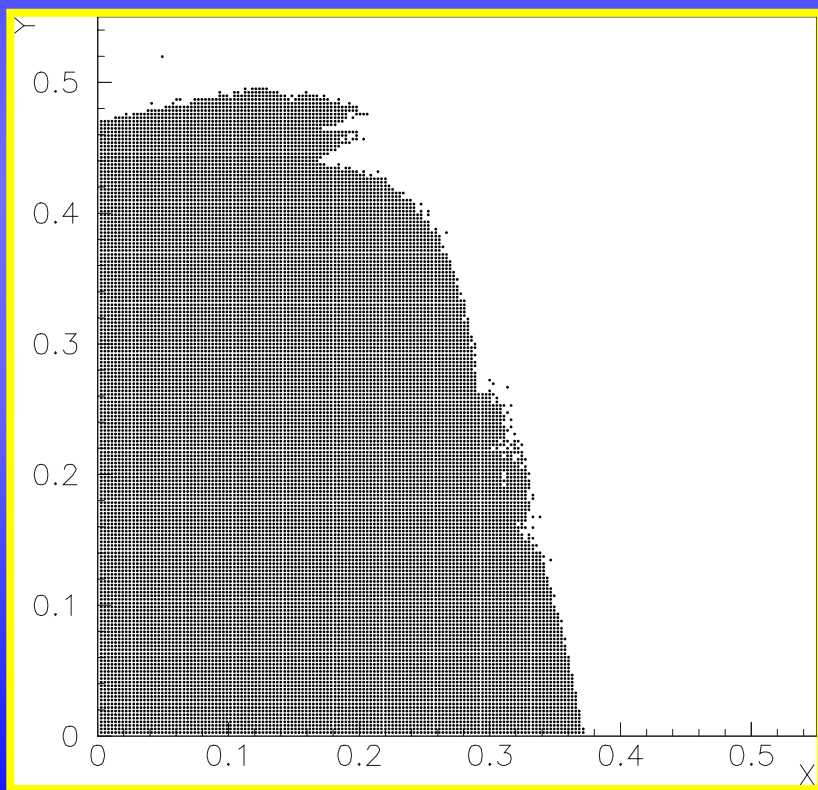
Direct DA computation 4/5

- ➡ This approach is not the unique solution to the problem of computing the volume integral:
- ➡ The scan in θ_1 , θ_2 (and the averaging step) is replaced by a *time average*. The underlying assumption is that the motion is *ergodic* (it might fail near low-order resonances). The power 4 in the scaling law for the error is replaced by a 2!
- ➡ Normal forms are used to compute the nonlinear invariant. This method has *same* behaviour (*error*) as previous one. Precautions should be taken for *convergence issues* (near low-order resonances).



Tracking examples: regular cases

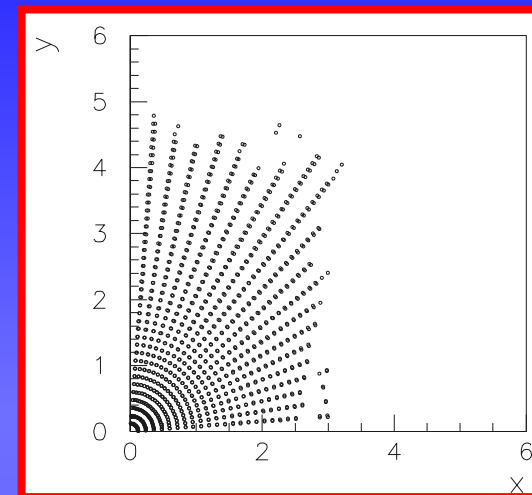
Henon map with octupoles and
 $v_x=0.28$, $v_y=0.31$. Initial
coordinates $(x,0,y,0)$.
 $N=1000$



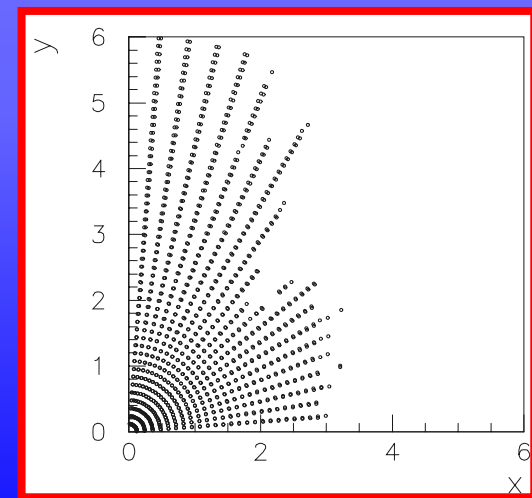
SPS model
with strong
sextupoles.

$v_x=26.637$,
 $v_y=26.533$.

$N=1000$



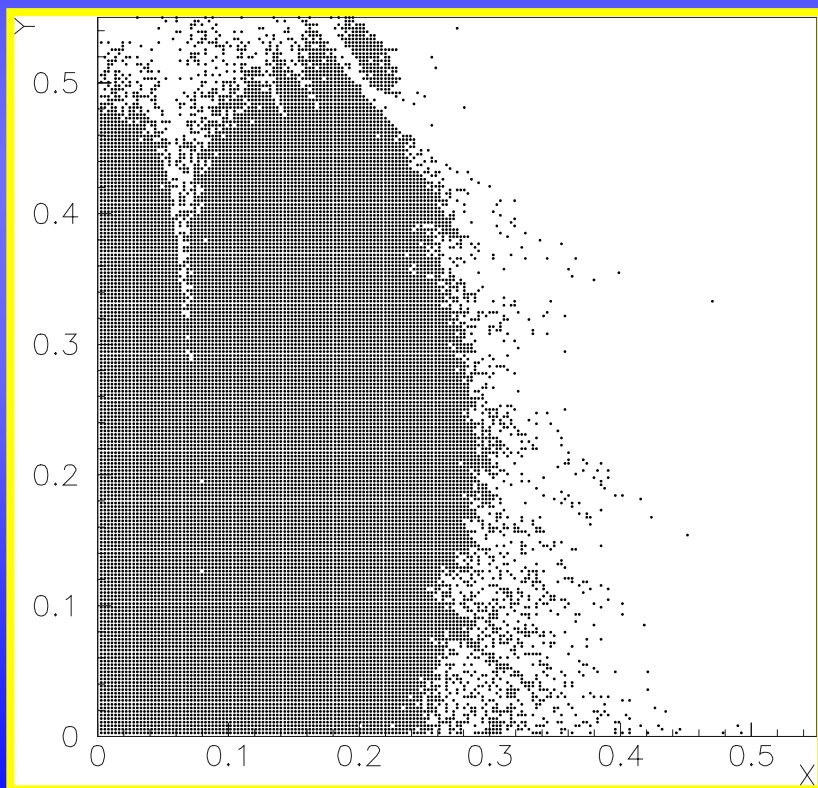
$v_x=26.605$,
 $v_y=26.538$.
 $N=1000$





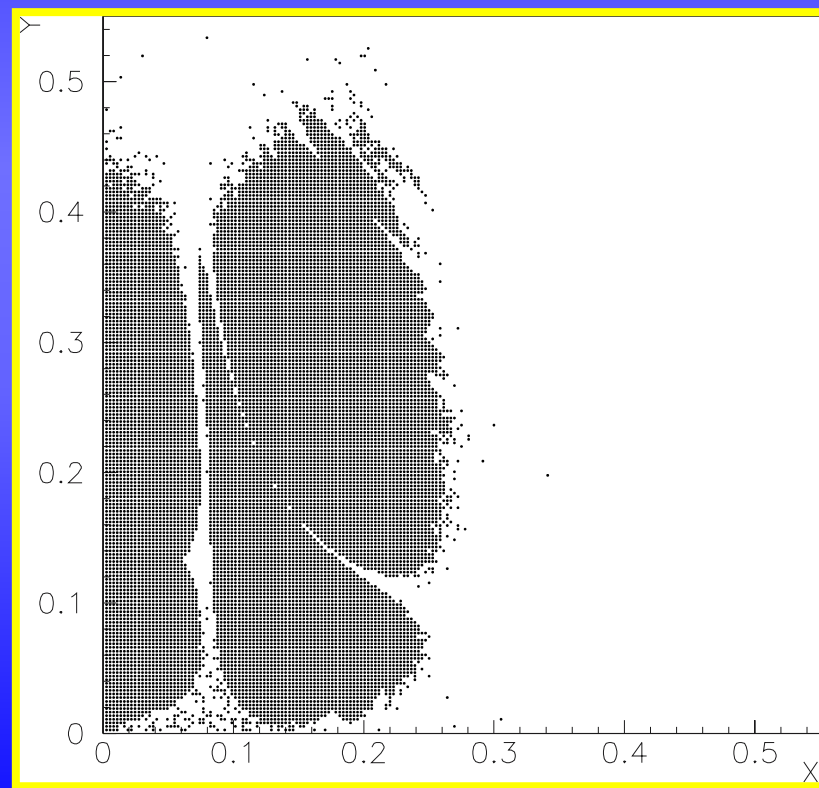
Tracking examples: pathological cases

Henon map with octupoles and
 $v_x=0.25$, $v_y=0.61803$. Initial
coordinates $(x,0,y,0)$.
 $N=1000$



Massimo Giovannozzi

Henon map with octupoles and
 $v_x=0.25$, $v_y=0.61803$. Initial
coordinates $(x,0,y,0)$.
 $N=50000$



HALO '03, May 21 2003

10



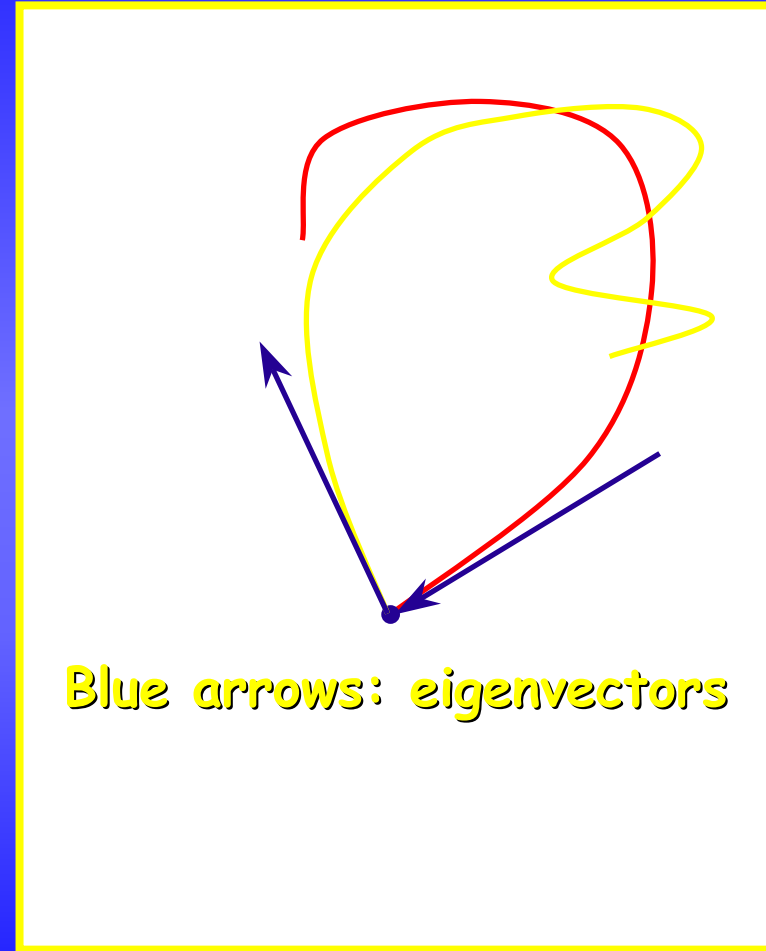
Direct DA computation 5/5

- ➡ How do we perform the tracking of initial conditions?
- ➡ The **Hamiltonian** character of the dynamics (for protons) makes it necessary to preserve **symplecticity**.
- ➡ Two approaches can be outlined:
- ➡ **Element-by-element tracking**: the **thick** nonlinear elements are replaced with **thin** lens kicks. The tracking is **exactly symplectic**, but the solution is an approximate one. However, **error** can be **controlled** exactly and **high-order** symplectic integrators are available.
- ➡ **Map tracking**: the polynomial map obtained by composition of the elements' map cannot be used directly (due to truncation errors). Hence, methods have been proposed to restore symplecticity, however, it is not clear whether **new physics** is added...



Semi-analytical computation of DA (2D) 1/4

- ➡ A semi-analytical method is based on **invariant manifolds**.
- ➡ From each hyperbolic fixed point emanates invariant manifolds tangent to the eigenvectors of the linearised map.
- ➡ These manifolds can be constructed numerically by iterating initial conditions on a small segment along the eigenvectors.





Semi-analytical computation of DA (2D) 2/4

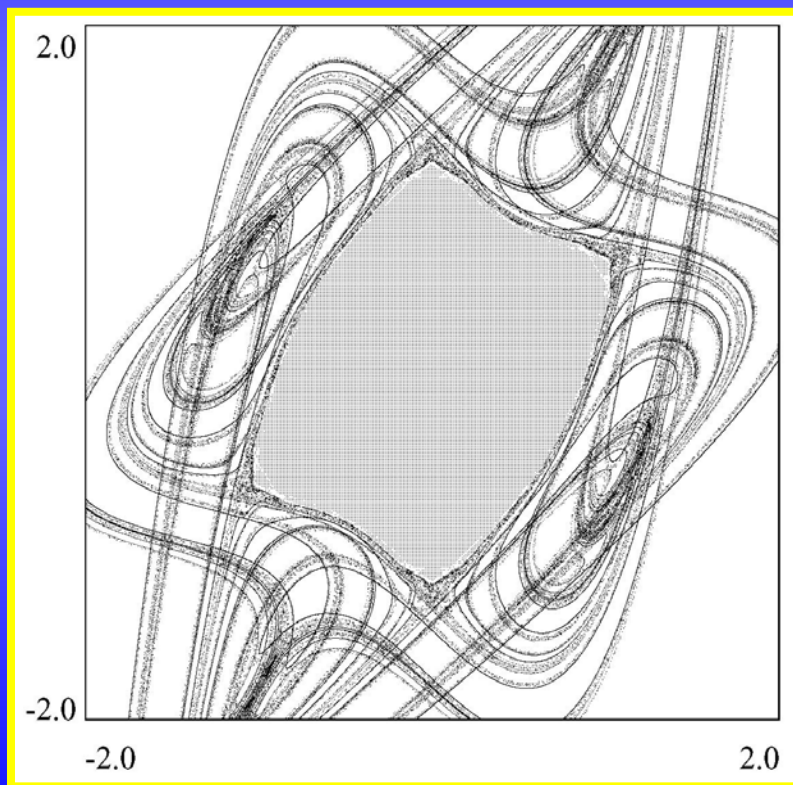
- ➡ Invariant manifolds emanating from different fixed points may intersect creating a complex structure (homoclinic/heteroclinic tangle).
- ➡ It has been shown that DA can be accurately computed using the following approach:
 - ➡ Find the lowest period (one or two) hyperbolic fixed point.
 - ➡ Determine eigenvectors of the linearised map.
 - ➡ Construct invariant manifolds emanating from that fixed point.
 - ➡ Compute the minimum distance from the origin: this will give the radius of the connected part of DA.

Essentially, intersections between the invariant manifolds from different unstable fixed points, will make the complex structure approaching the border of stability from outside.

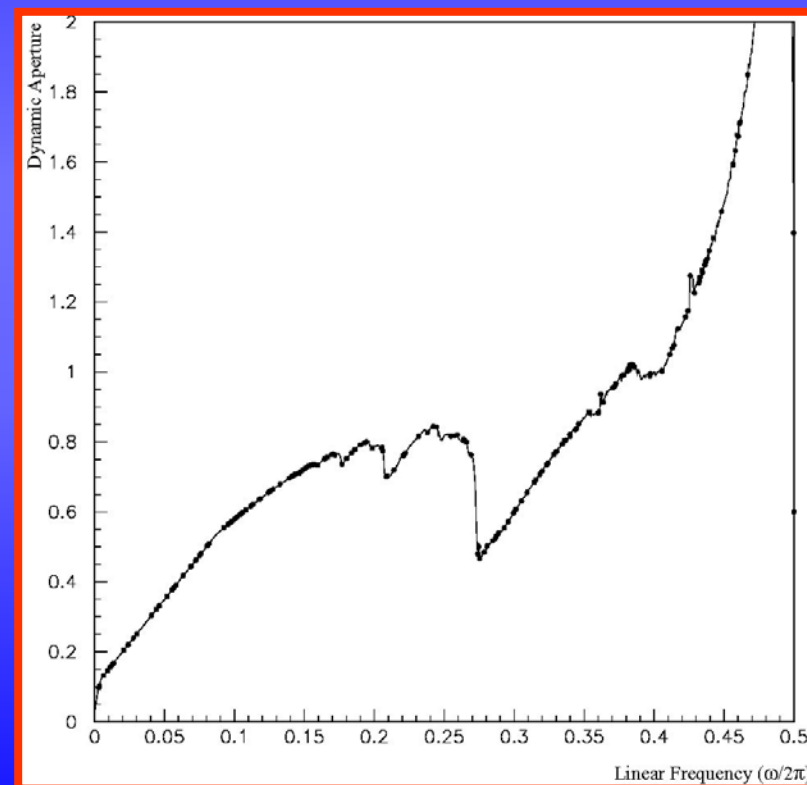


Semi-analytical computation of DA (2D) 3/4

Invariant manifolds form the hyperbolic points of period one for the cubic map ($\nu_x=0.34$). The stability domain is also shown.

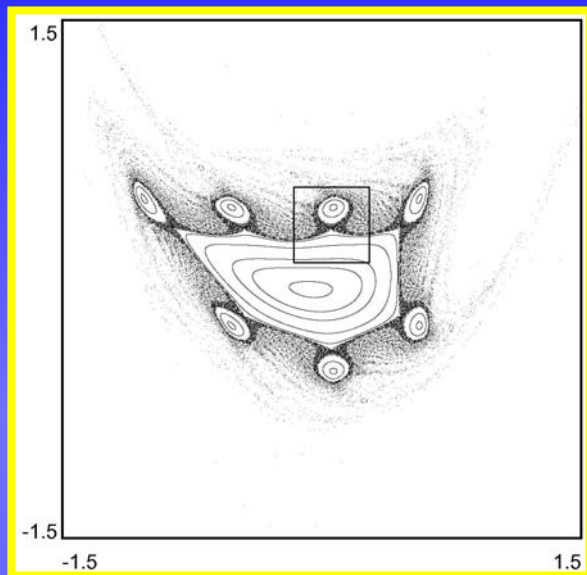


Global behaviour of the dynamic aperture for the cubic polynomial map

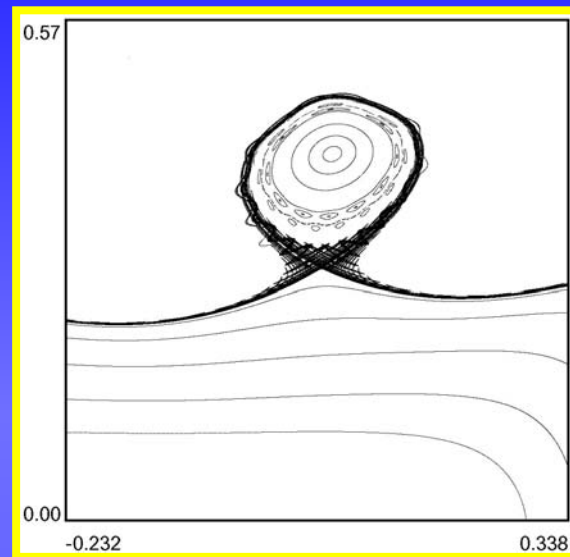




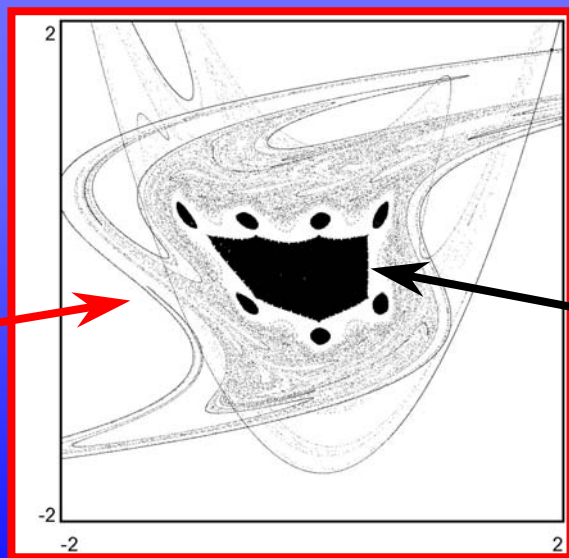
Semi-analytical computation of DA (2D) 4/4



Orbits of a nonlinear polynomial map



Invariant manifolds



Stability domain



Early indicators 1/4

- ➡ The goal is to find **dynamical observables**, to be computed easily, over a **limited number of turns**, showing a **good correlation** with **long-term stability**!
- ➡ Outstanding issues
 - ➡ **Intermittency**: particles showing a stable behaviour over 10^3 - 10^4 turns, suddenly escape to infinity. No remedy seems to be available to deal with such a situation.
 - ➡ **Stable chaos**: initial conditions showing a **highly chaotic dynamics** are **not lost** over a **large number** of turns. No result is available to prove that chaotic particles will be lost anyway...



Early indicators 2/4

- ➡ **Bounds on invariants**
- ➡ The approach is based on an accurate computation of the invariants.
- ➡ Based on this, the maximum variation of the invariant δJ in the accessible region of phase space is computed (Monte Carlo) for a given number of turns n_0 .
- ➡ Stability times are derived via (ΔJ is a parameter)

$$N = \frac{\Delta J}{\delta J} n_0$$



Early indicators 3/4

► Lyapunov exponent

$$\lambda(N) = \frac{1}{N} \log \left| \frac{x^{(N)} - \hat{x}^{(N)}}{\delta} \right| \quad \delta \ll 1$$

► A threshold is defined using numerical simulations of a simple model (Henon map)

$$\sigma_\lambda(N) = \frac{1}{N} \log(N A_\lambda) \quad A_\lambda = 0.15$$

► Particles satisfying

$$\lambda(N) \geq \sigma_\lambda(N) \text{ are unstable}$$



Early indicators 4/4

► Tune variation

$$\tau(N) = \sqrt{\frac{1}{2} \sum_{i=x,y} [\nu_i(1:N/2) - \nu_i(N/2+1:N)]^2}$$

► A threshold is defined using numerical simulations of a simple model (Henon map)

$$\sigma_\tau(N) = \frac{A_\tau}{N} \quad A_\tau = 0.2$$

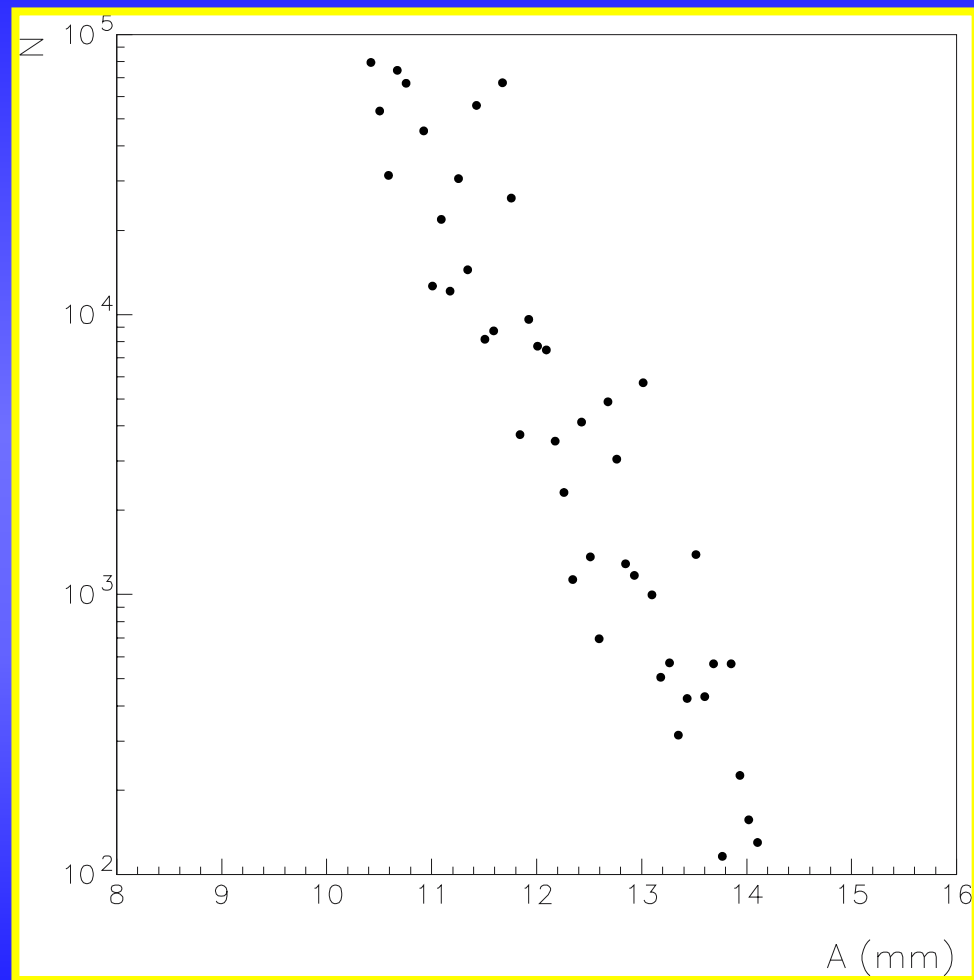
► Particles satisfying

$$\tau(N) \geq \sigma_\tau(N) \text{ are unstable}$$



Inverse Logarithm Interpolation 1/4

- ➡ Results of numerical evaluation of DA can be presented in different forms.
- ➡ It is customary to use the so-called *survival plots*: DA is plotted against the number of turns.
- ➡ If DA is computed using too few angles, α , and/or without applying the proposed averaging, the survival plots do not convey all the possible information.

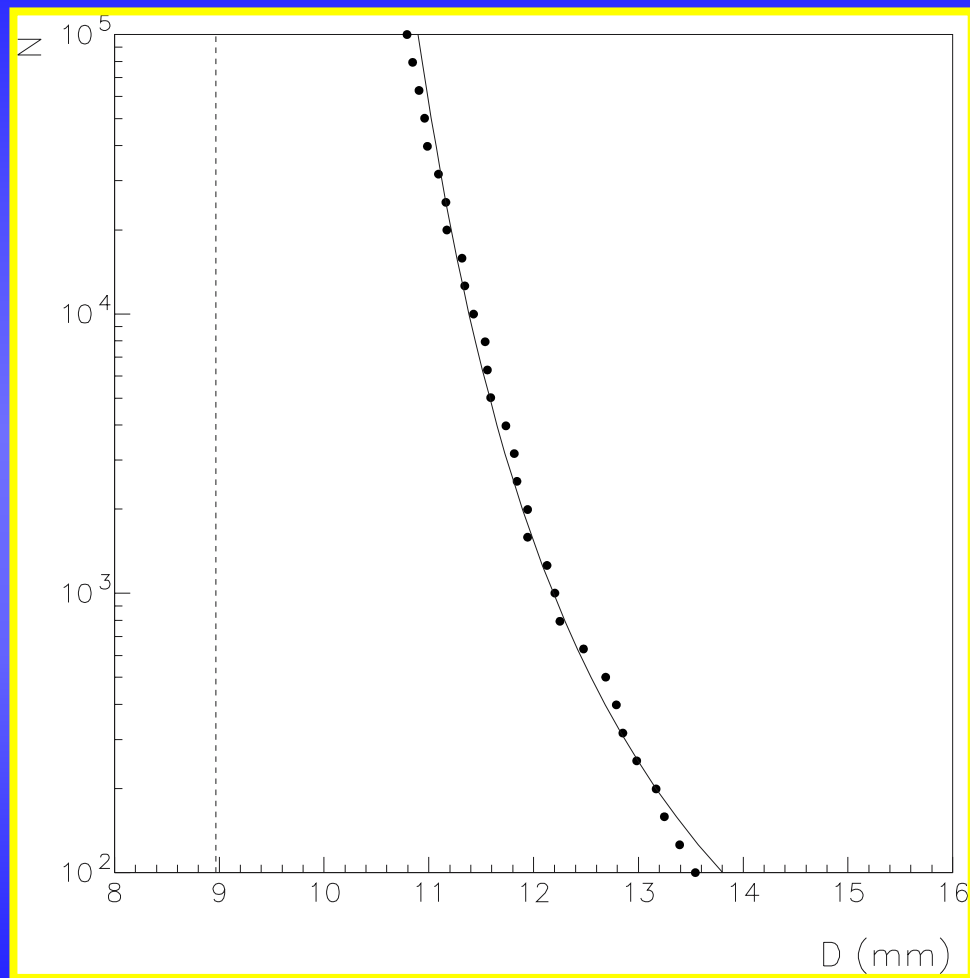




Inverse Logarithm Interpolation 2/4

- ➡ If the DA, computed using the approach presented before, is plotted against the number of turns a smooth curve appears!
- ➡ It turns out the it can be fitted by the following law:

$$D(N) = D_{\infty} \left[1 + \frac{b}{\log(N)} \right]$$





Inverse Logarithm Interpolation 3/4

$$D(N) = D_{\infty} \left[1 + \frac{b}{\log(N)} \right]$$

- ➡ Some comments:
- ➡ The scaling law depends on two parameters only!
- ➡ They have a clear physical meaning:
- ➡ D_{∞} : it represents the DA at "*infinite time*". It is the limiting value of DA.
- ➡ b : gives the relative importance between short-term and long-term DA.
- ➡ The scaling law has been tested also for 6D motion in realistic models (LHC lattice).



Inverse Logarithm Interpolation 4/4

- ➡ There is an interesting connection with fundamental theorems such as **KAM** and **Nekhoroshev**.
- ➡ By inverting the relation stating the dependence of the stability time on the amplitude (**Nekhoroshev**) one obtains

$$r(N) = \frac{R}{\log^{1/A}(N / N_0)}$$

- ➡ The **KAM** theorem is applied to support the statement that diffusion is practically **negligible**, at least **not too far from the origin**, thus ensuring the existence of a stable region of radius r_∞ , then particles beyond r_∞ escape according to

$$r(N) = r_\infty + \frac{R}{\log^{1/A}(N / N_0)}$$



Comparison of DA calculations

LHC 4D

N	Particle Loss	Lyapunov	Tune	Extrapolation 10 ⁷	∞
128	24 %	4 %	-4 %		
512	17 %	-12 %	0 %	3 %	-6 %
2048	11 %	-13 %	-4 %	-6 %	-21 %
8192	6 %	-15 %	-6 %	-4 %	-17 %
10 ⁵	0 %			-5 %	-19 %

LHC 6D

128	39 %	12 %			
512	29 %	9 %		-1 %	-20 %
2048	21 %	0 %	-4 %	-2 %	-21 %
8192	13 %	-6 %	-7 %	-2 %	-21 %
10 ⁵	0 %			-7 %	-31 %



Time-dependent effects 1/4

- ➡ Real machines are plagued by **time-dependent** effects, e.g. **ripple** in the power supplies, **persistent currents** (superconducting machines).
- ➡ This generates **tune modulation**.
- ➡ Tune can be modulated also by **synchro-betatron** coupling.
- ➡ A complex phenomenology arises: phase space topology depends on **mutual interaction** of parameters, i.e. linear tunes, amplitude and frequency of tune modulation.



Time-dependent effects 2/4

- ➡ In general the performance of early indicators get worse in presence of tune modulation.
- ➡ Lyapunov exponent provides very pessimistic estimates of DA due to the large scale chaotic motion.
- ➡ How does the inverse logarithm interpolation behave in presence of tune modulation?



Time-dependent effects 3/4

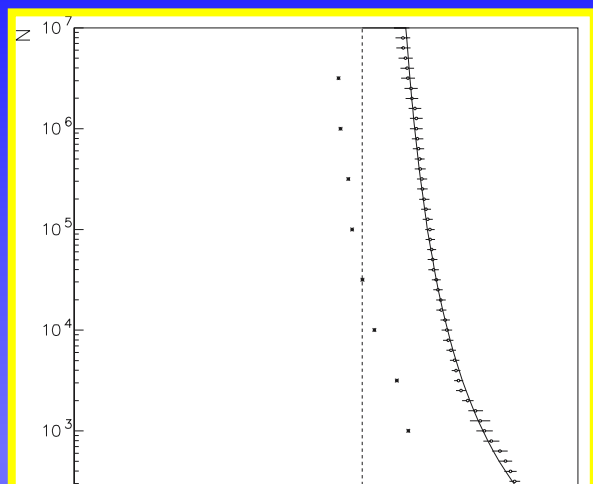
- ➡ The following form of the interpolating function was chosen

$$D(N) = A + \frac{B}{\log^{\kappa}(N)}$$

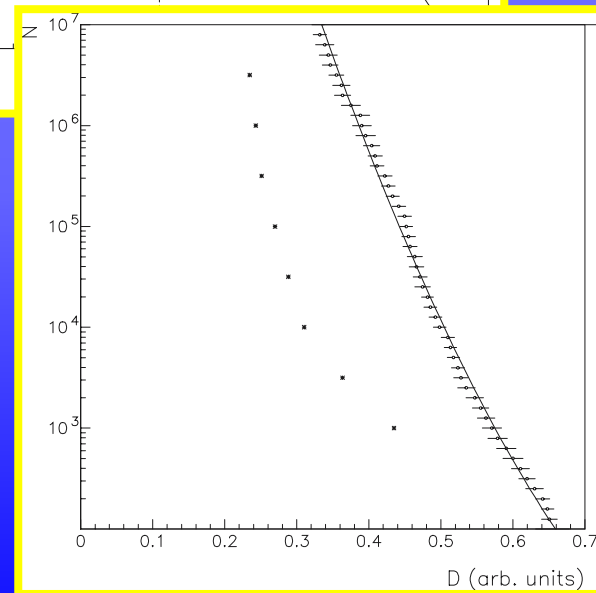
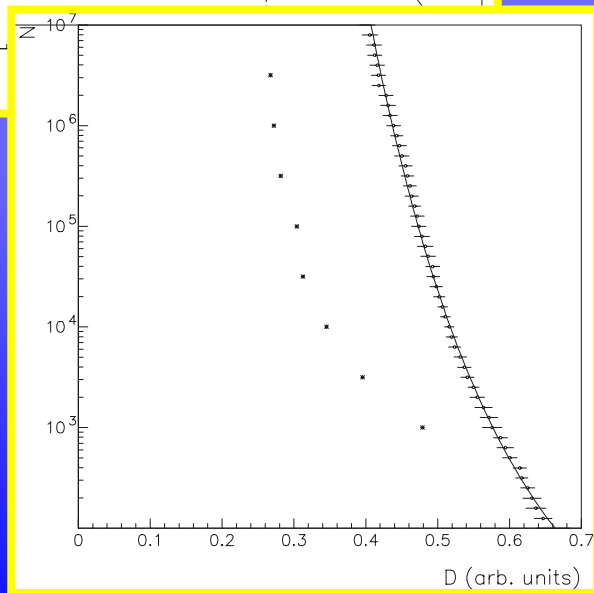
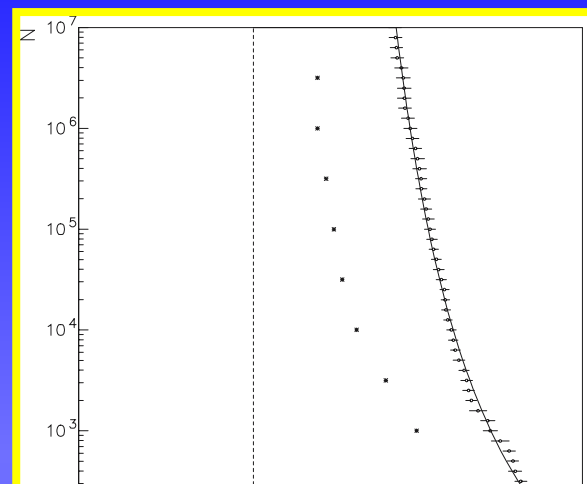
- ➡ Strictly speaking, in presence of tune modulation Nekhoroshev theorem does not hold (**modulation is not a weak perturbation**).
- ➡ From a phenomenological point of view tune modulation induces strong long-term effects.
- ➡ **A posteriori: the fit quality is always very good!**
- ➡ In presence of strong modulation κ (or A) becomes **negative**: the entire phase space is unstable.



Time-dependent effects 4/4



DA simulations
for Henon
modulated map



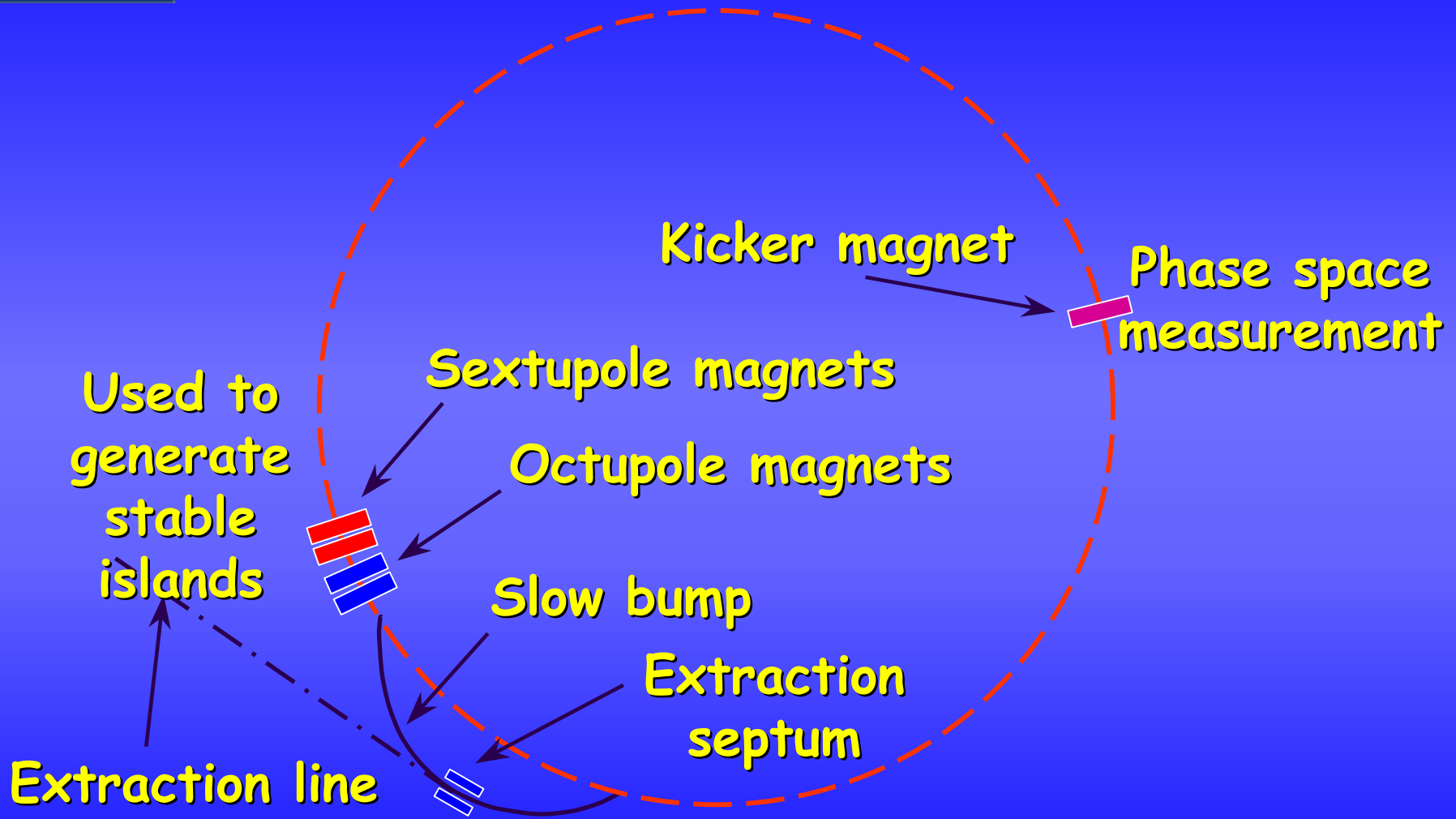


Nonlinear dynamics experiments

- ➡ On the experimental front, considerable efforts were devoted to test some outstanding issues related to nonlinear beam dynamics.
- ➡ These measurements were aimed at determining quantities such as **detuning** with amplitude, **smear**, **islands'** parameters (size, position).
- ➡ In some cases **DA** measurements were attempted, including its parametric dependence (on ripple, for instance).



Phase space reconstruction 1/2

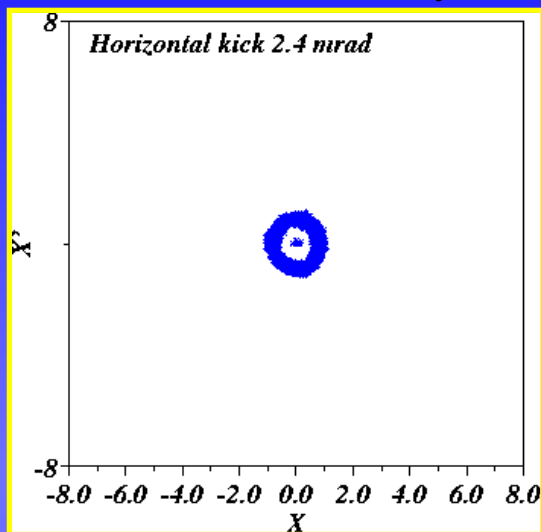




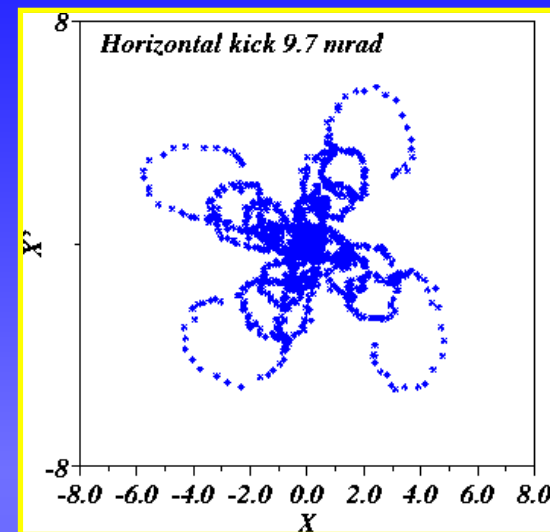
Phase space reconstruction 2/2

Measurement performed at the CERN PS in 2002

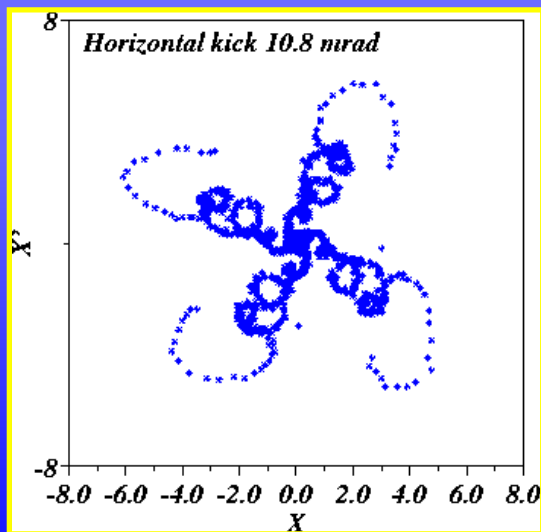
Regular
motion near
the origin of
phase space



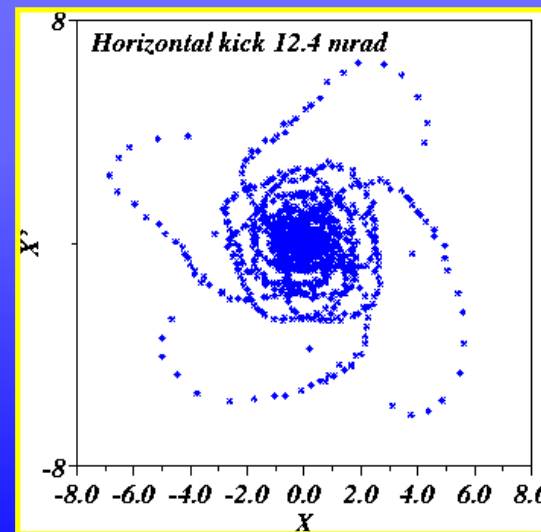
Motion
inside
islands



Motion
inside
islands



Motion
beyond
islands'
separatrix





Nonlinear dynamics experiments: FNAL E778

➡ Machine conditions:

- ➡ Tevatron at injection.
- ➡ Dedicated **sextupoles** are used to create nonlinear effects.
- ➡ The tune is near $\nu_x = 2/5$.

➡ Measurements:

- ➡ **Smear**.
- ➡ **Detuning** with amplitude.
- ➡ **Evolution** of beam **profiles**.
- ➡ Islands properties (including trapping efficiency vs. tune modulation parameters).
- ➡ **DA**: reasonable agreement with tracking (**20 %**).



Nonlinear dynamics experiments: DESY HERA-p

➡ Machine conditions:

- ➡ HERA-p at injection (after decay of persistent currents).
- ➡ Nonlinear effects are the natural ones due to superconducting magnets.

➡ Measurements:

- ➡ **Detuning** with amplitude (used to cross-check the model).
- ➡ **Tune ripple** (including the possibility of correcting the ripple).
- ➡ **DA**: it was measured using two different methods.



Nonlinear dynamics experiments: DESY HERA-p

- ➡ Beam profiles: 1) the beam is kicked; 2) the width of the beam profile is measured after some time.
- ➡ Beam losses: 1) the beam is scraped; 2) scrapers are retracted; 3) the beam is kicked to sample a given amplitude.
- ➡ Observations:
 - ➡ The control of experimental conditions in the vertical plane is rather difficult.
 - ➡ At injection the influence of ripple is negligible.
 - ➡ At top-energy ripple effects are relevant.
 - ➡ Scraper measurements agree with a diffusion model at top-energy, but not at injection.
 - ➡ DA: a 20 % agreement with tracking was achieved.



Nonlinear dynamics experiments: CERN SPS

➡ Machine conditions:

- ➡ SPS at 120 GeV (the machine is very linear).
- ➡ Eight sextupoles are powered to excite nonlinear resonances (but not the third-order).
- ➡ Octupoles are used to reduce the detuning (by product of these measurements: the correction of the tunes is beneficial for the dynamics).

➡ Measurements:

- ➡ Detuning with amplitude (used to cross-check the model).
- ➡ Tune ripple.
- ➡ DA: it was measured using beam losses.



Nonlinear dynamics experiments: CERN SPS

► Observations:

- The lack of a real pencil beam is believed to be the major obstacle (and limiting factor) for this measurement.
- No dependence of DA on ripple (**artificially introduced**) frequency emerged from the measurements.
- The presence of a second frequency has a negative impact on the beam stability.
- **DA**: a **20 %** agreement with tracking was achieved.



Conclusions 1/2

- ➡ Although a definitive solution to the problem of computing efficiently and correctly DA is not at hand, yet, a number of results have been obtained:
 - ➡ Various approaches have been proposed to compute the connected volume of stable initial conditions in phase space (DA).
 - ➡ The dependence of the error on computed DA is known, thus allowing for an optimal choice of the grid step.
 - ➡ Early indicators have been defined, and their properties studied in details.
 - ➡ An interpolation law has been worked out: it allows a reliable extrapolation of tracking results.



Conclusions 2/2

- ➡ Nonlinear dynamics experiments have been performed at **FNAL (E778)**, **DESY (HERA-p)**, **CERN (SPS)**.
 - ➡ A **good** agreement with tracking results was found for **detuning with amplitude, smear, and islands properties**.
 - ➡ Whenever the experimental conditions are well under control, the agreement between **DA** measurements and tracking is of the order of **20 %**.



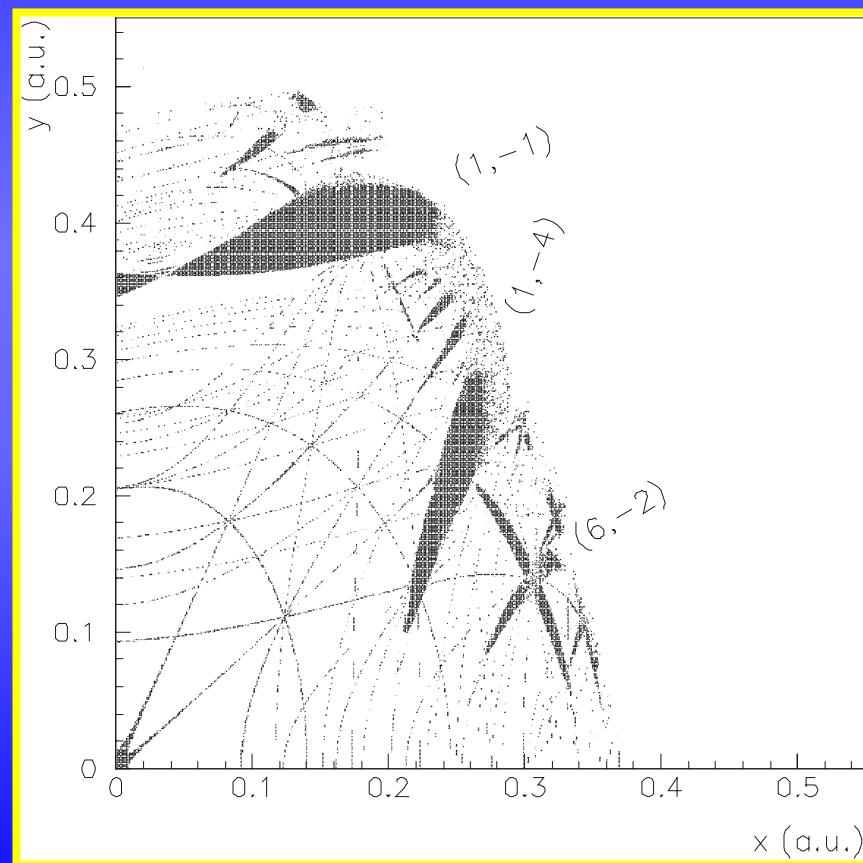
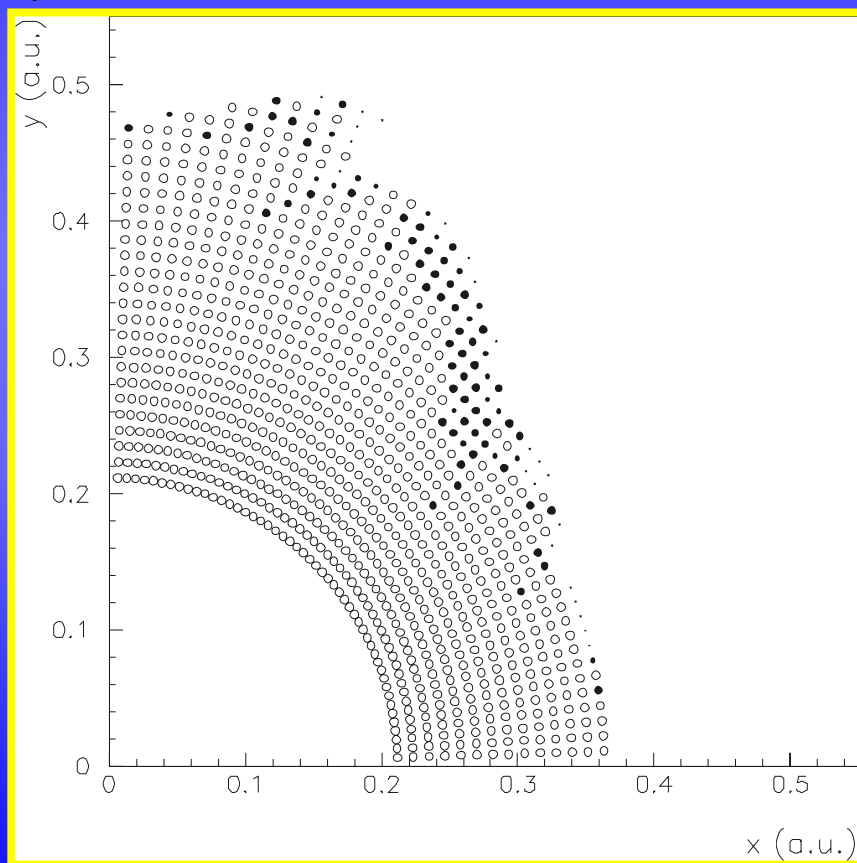
Acknowledgements

- ➡ I am particularly in debt with **G. Turchetti** who introduced me in this field. He was the first to point out the deep implications of the logarithm interpolation.
- ➡ Most of the results on computation of DA represent a joint effort with **E. Todesco** and **W. Scandale**.
- ➡ **W. Fischer** and **F. Schmidt** are gratefully acknowledged for the collaboration during the SPS experiment (tracking studies, long night-shifts in control room).
- ➡ **F. Zimmermann** pointed out a number of references concerning nonlinear dynamics, and DA measurements.
- ➡ The colleagues of the Accelerator Physics group at CERN for discussions.



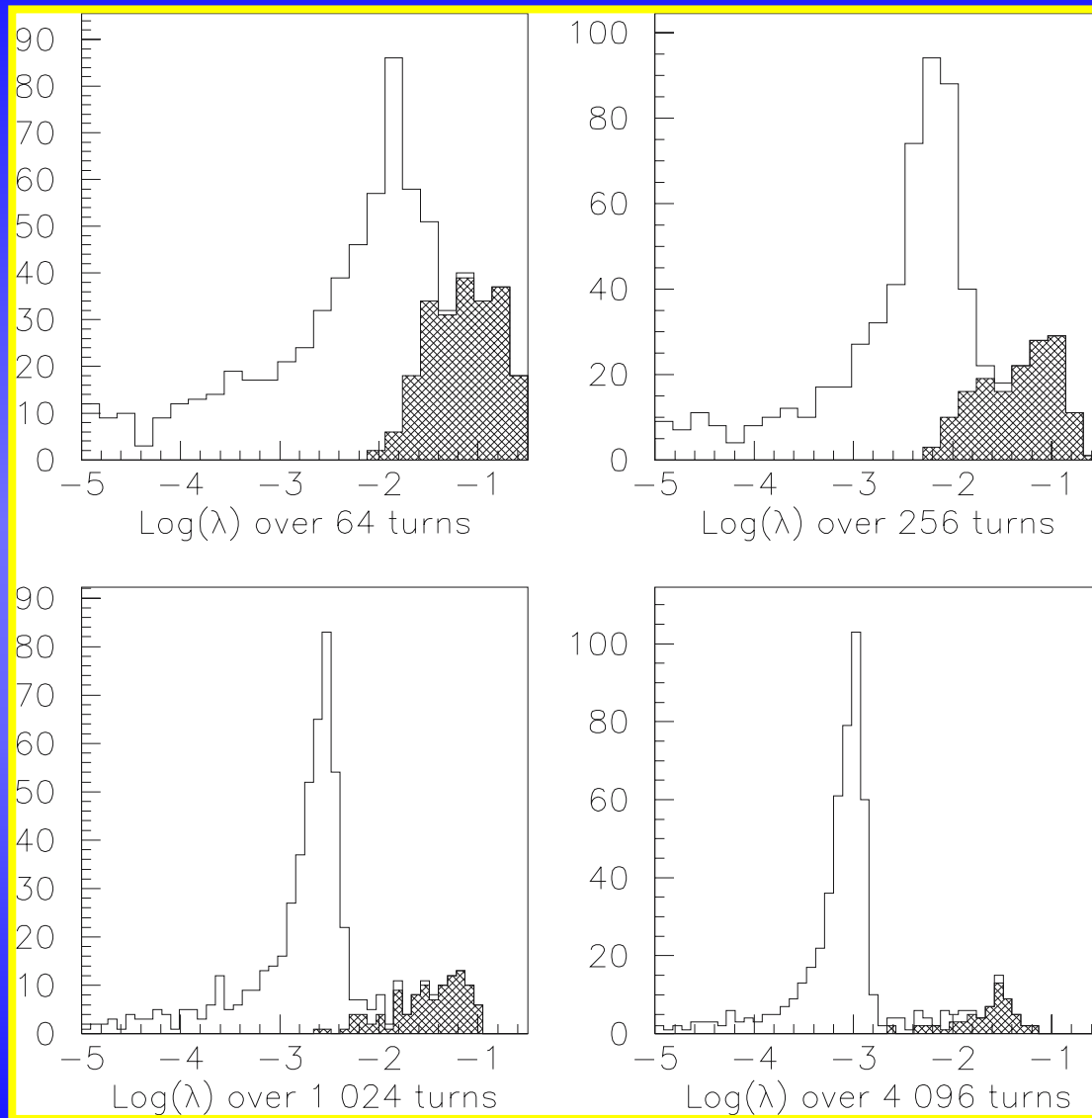
Tracking examples: regular cases

Henon map with octupoles and $v_x=0.28$,
 $v_y=0.31$. Initial coordinates $(x,0,y,0)$.
 $N=10^7$





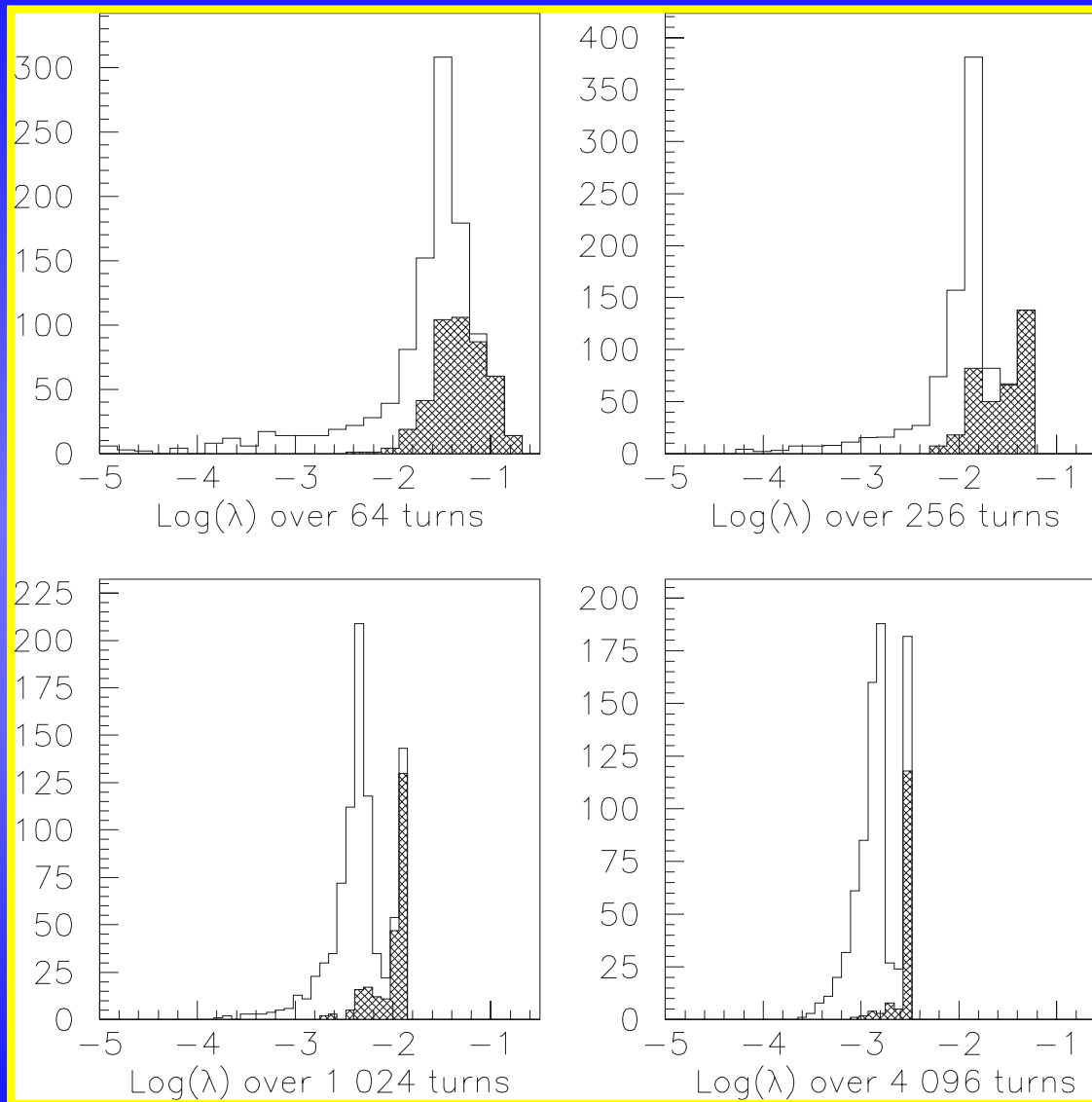
Early indicators 3/5: Henon



Particles lost before 10^7 turns are marked in black (Henon map).



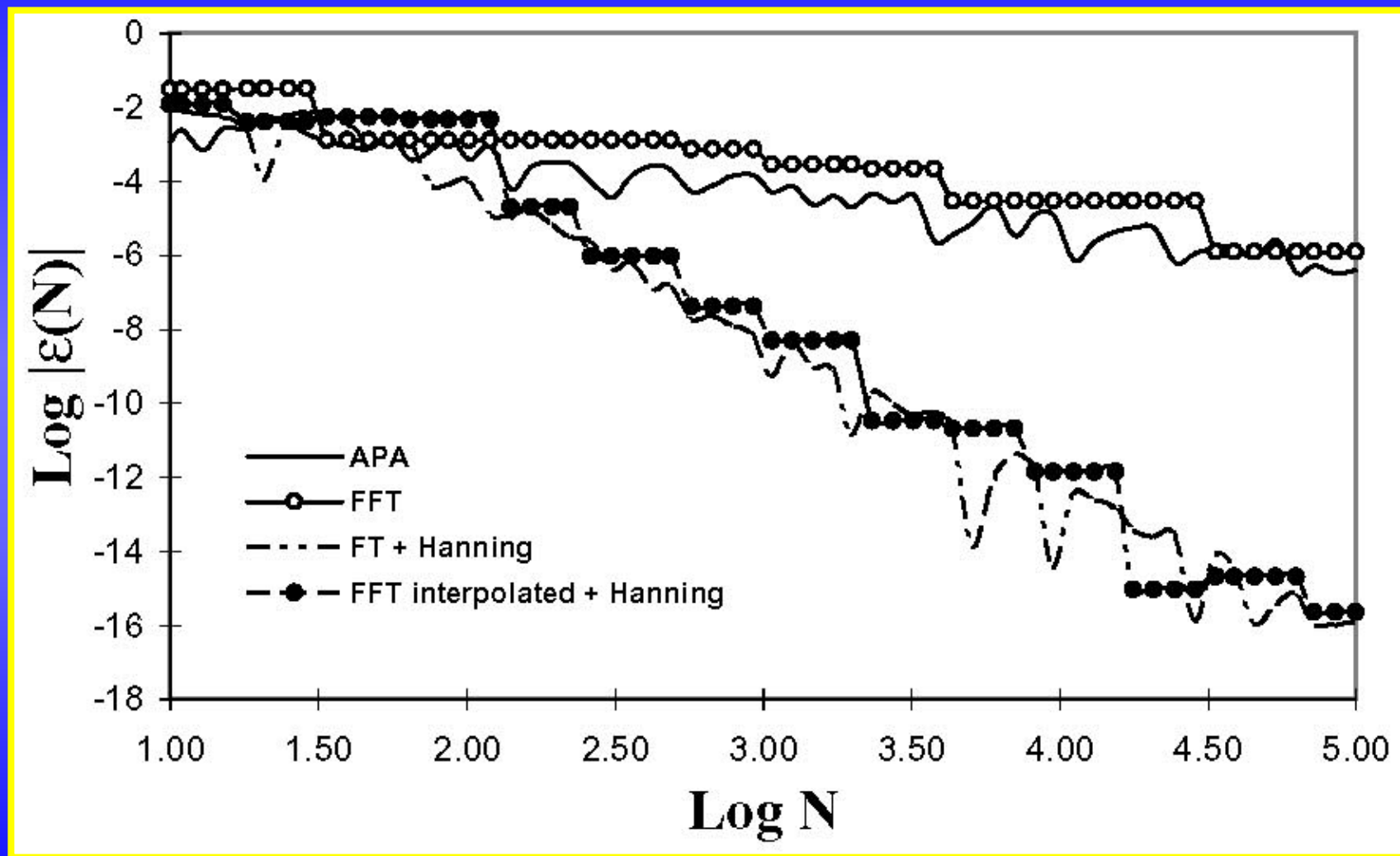
Early indicators 3/5: LHC



Particles lost before 10^7 turns are marked in black (LHC model).



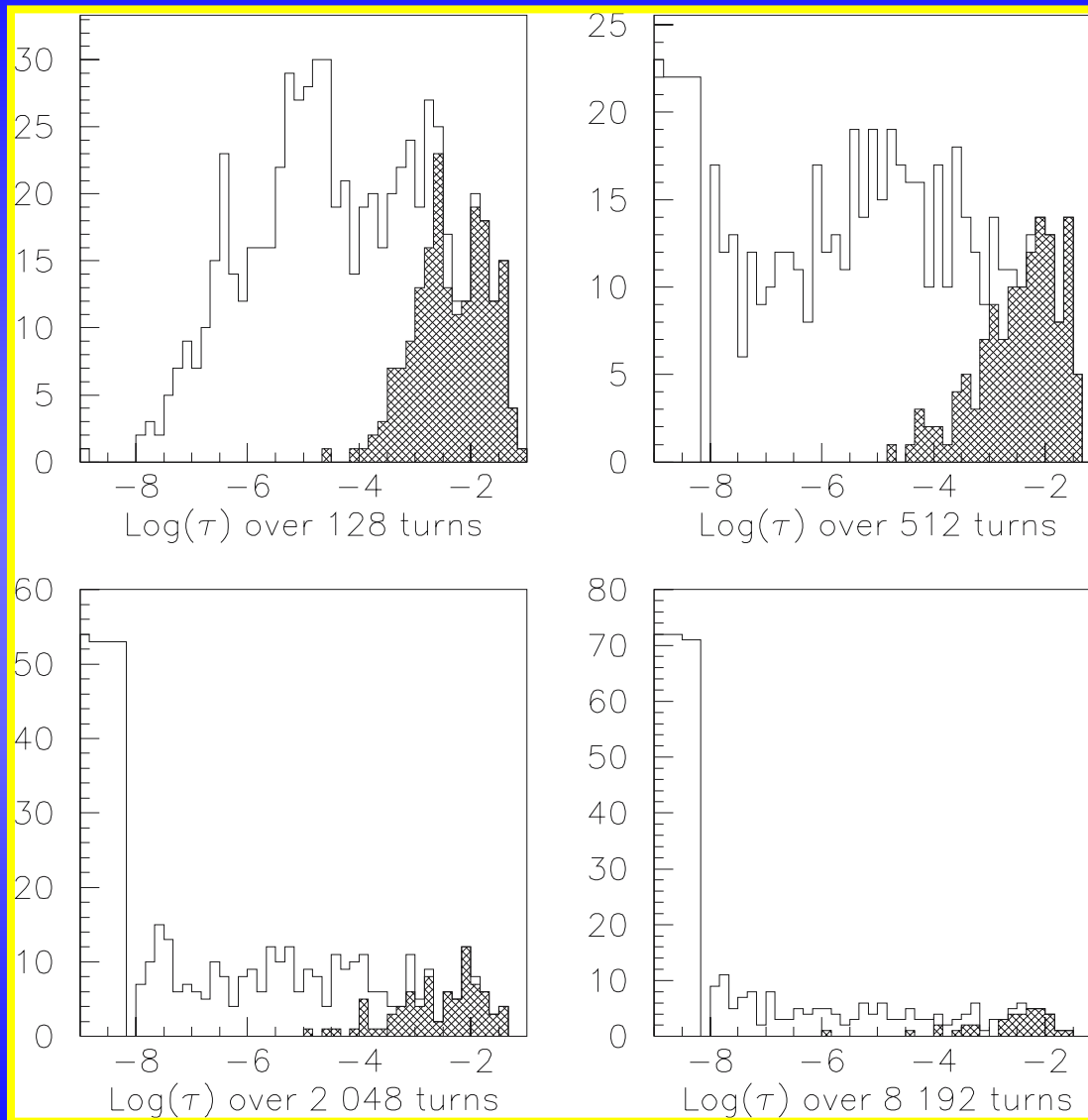
Harmonic analysis of time-series





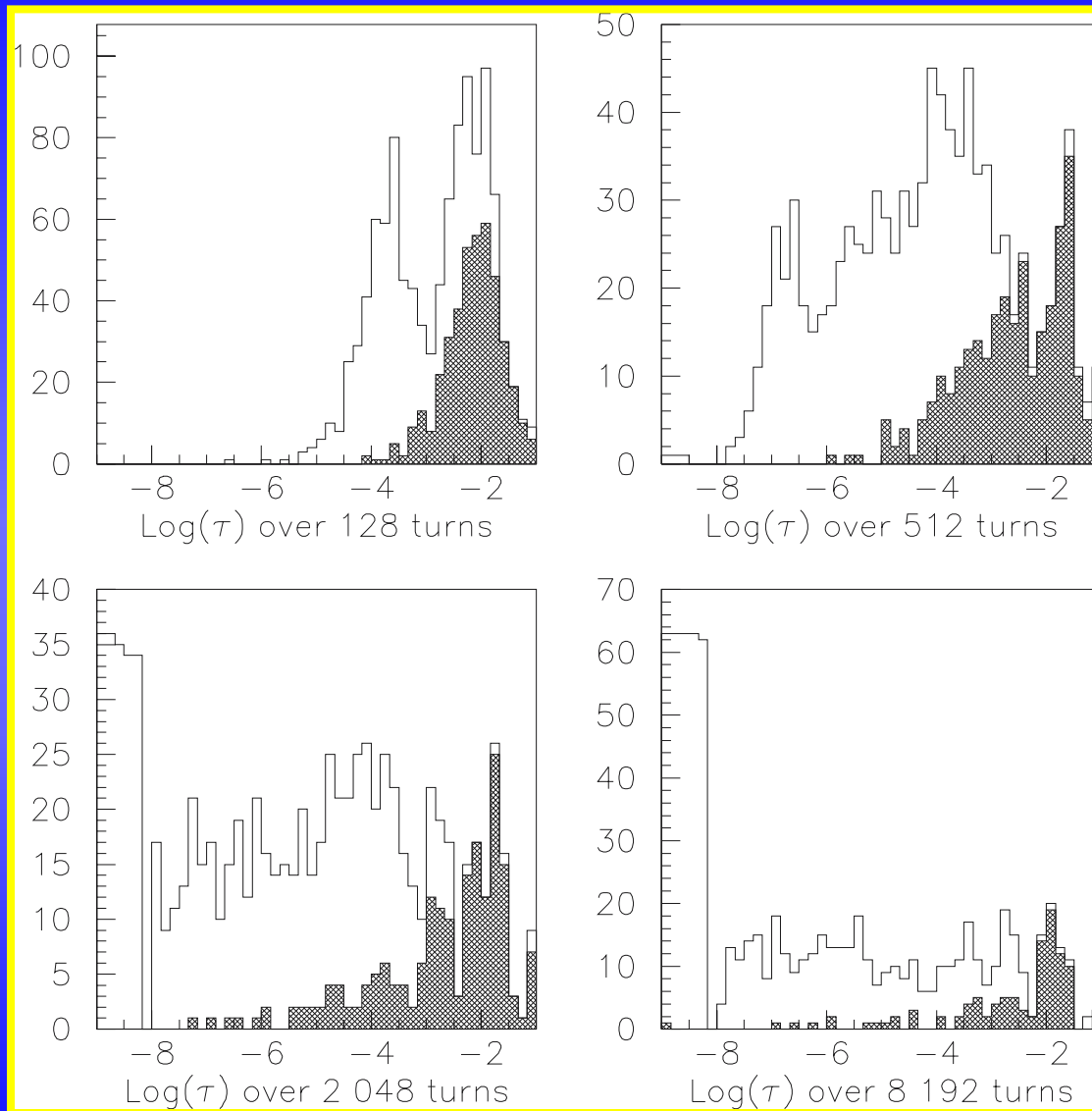
Early indicators 4/5: Henon

Particles lost
before 10^7
turns are
marked in black
(Henon map).





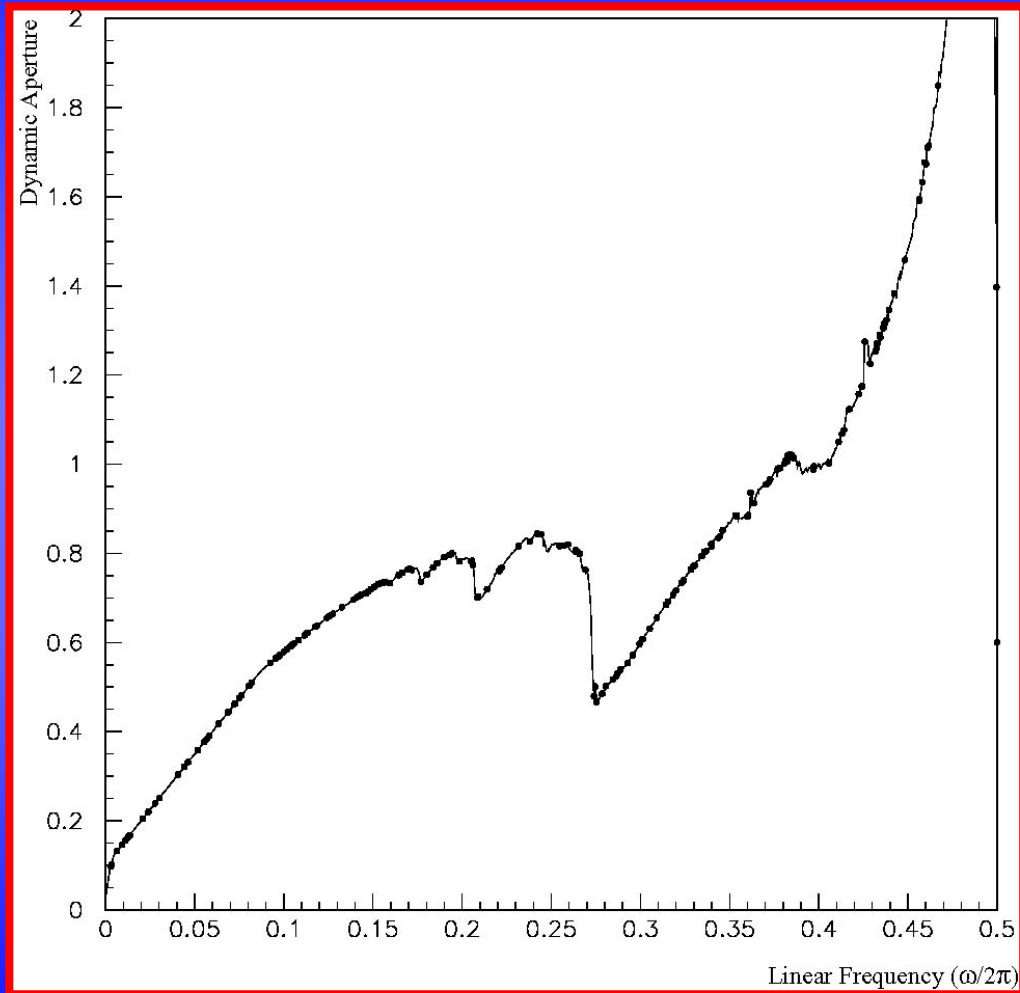
Early indicators 4/5: LHC



Particles lost before 10^7 turns are marked in black (LHC model).



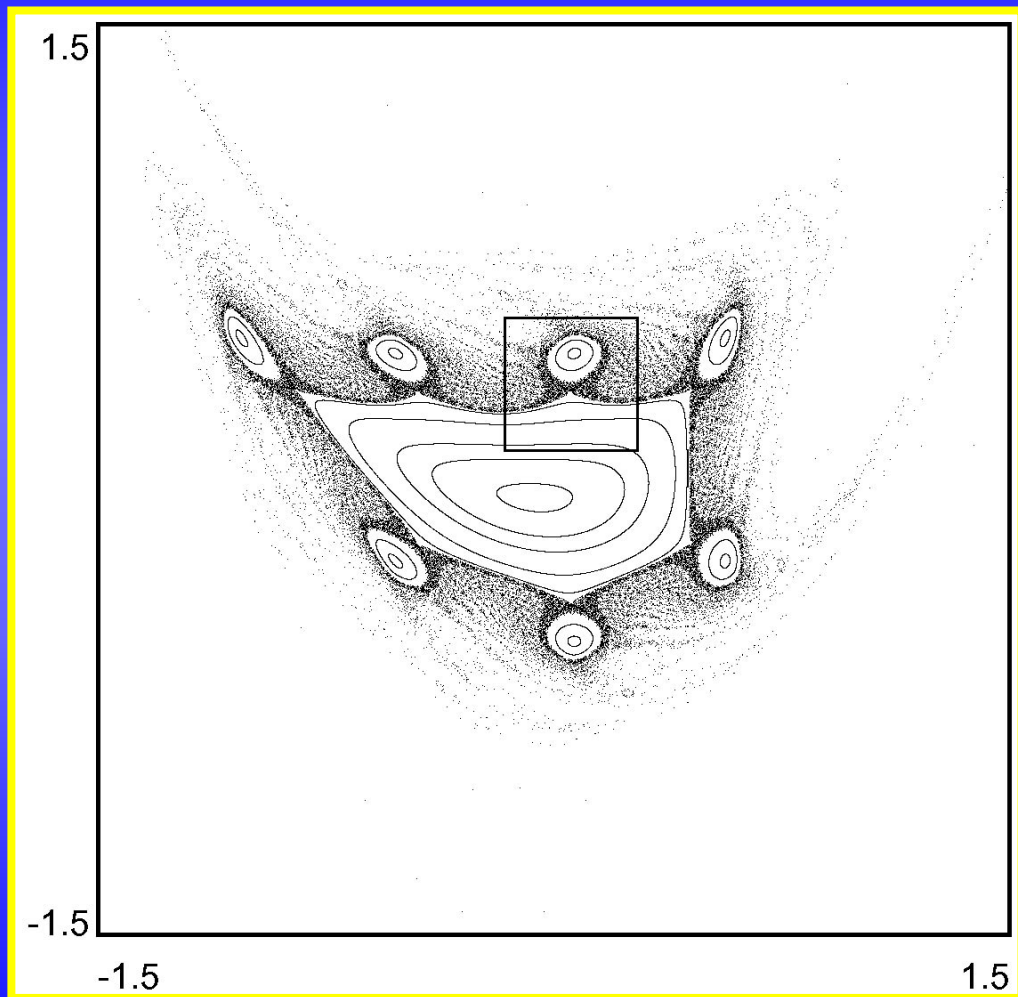
Semi-analytical computation of DA (2D) 1/3



- ➡ A polynomial map of order three is used.
- ➡ Dynamic aperture (radius of the stability domain) vs. linear tune (solid line).
- ➡ Minimum distance of the inner envelope of the homoclinic tangle (dots).



Semi-analytical computation of DA (2D) 3/3



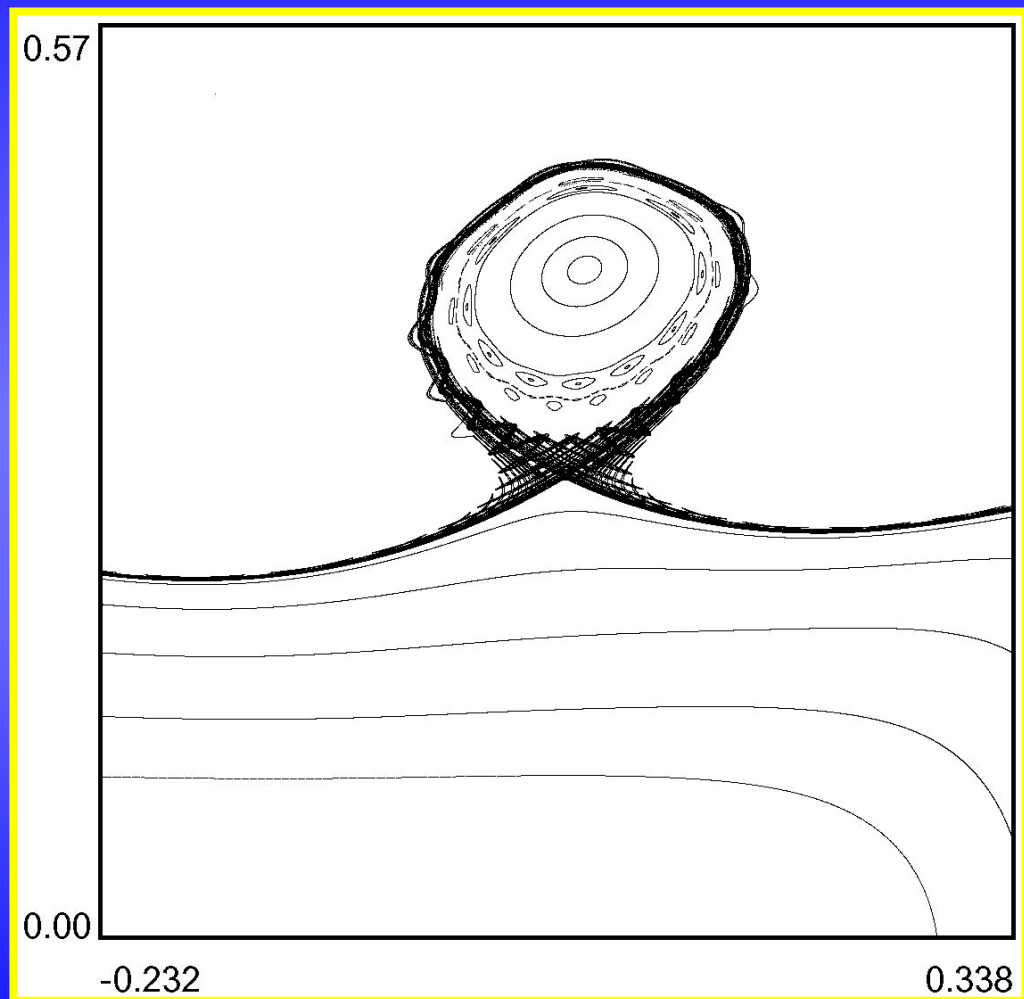
◆ Orbits of a polynomial map of order 6.

◆ Island chain of period 7 is clearly visible.

◆ A thick stochastic layer is also visible.



Semi-analytical computation of DA (2D) 3/3

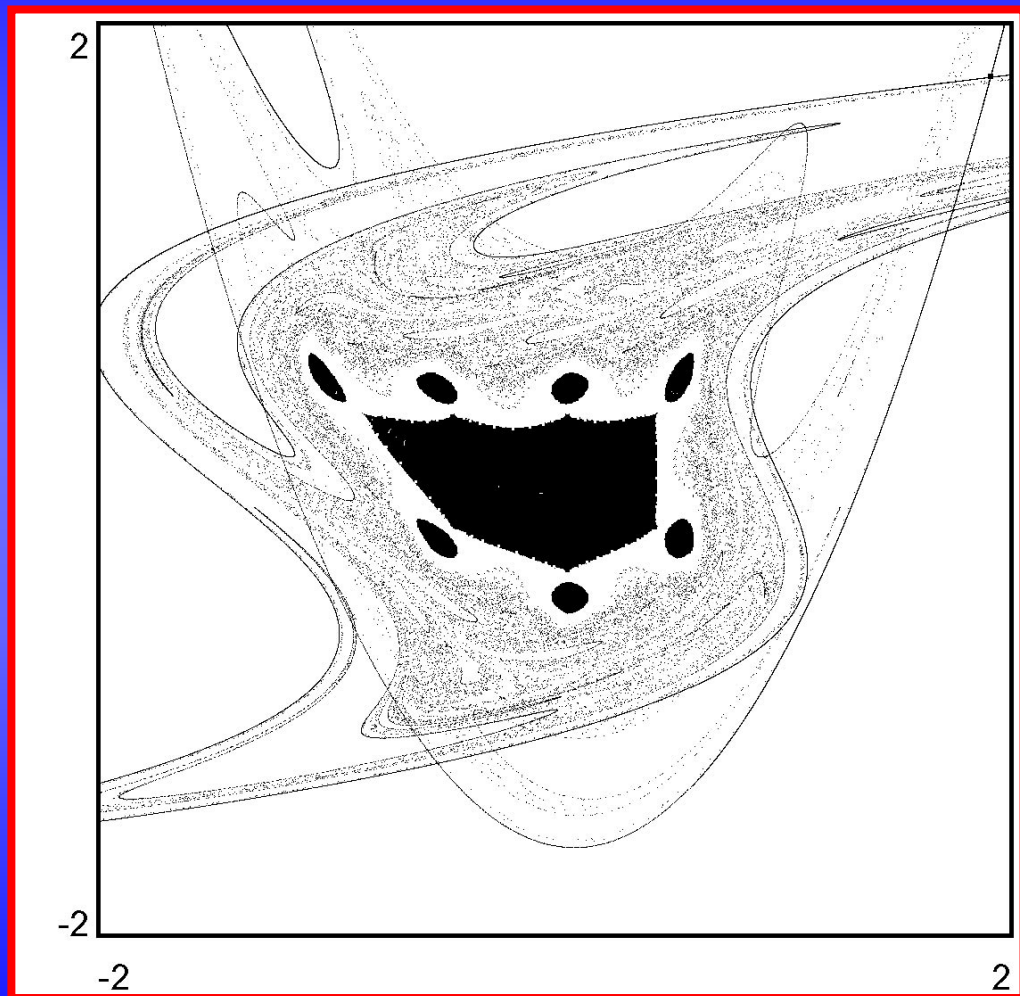


◆ Detail of one islands of period 7.

◆ Higher-period islands are visible inside.

◆ The homoclinic tangle is clearly visible.

Semi-analytical computation of DA (2D) 3/3

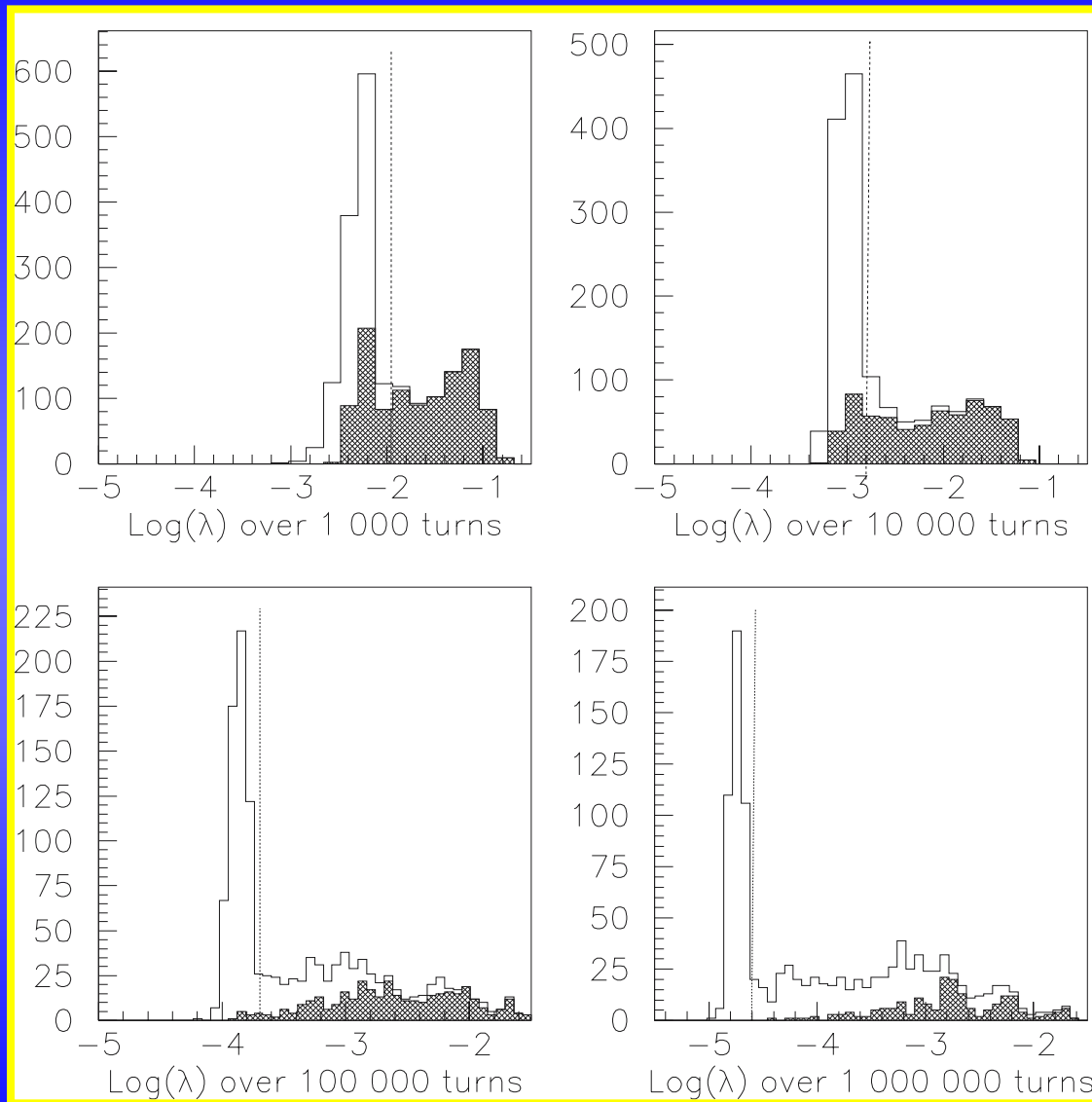


◆ Stability domain for the polynomial map of order 6. It is obtained by direct tracking.

◆ The invariant manifold emanating for the hyperbolic fixed point of period one is shown.



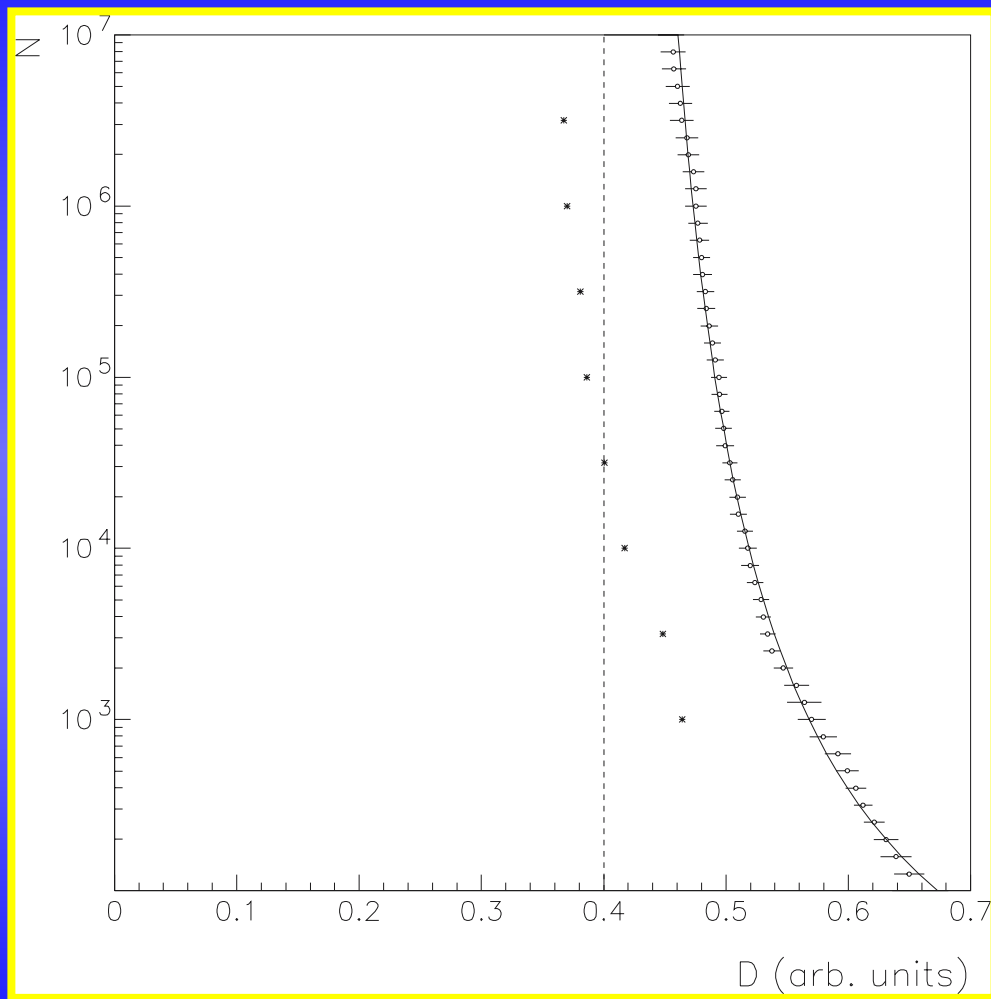
Time-dependent effects 2/4



Distribution of
Lyapunov
exponent for
modulated
Henon map.
Particles lost
before 10^7
turns are
marked in black



Time-dependent effects 4/4



Simulation results for
modulated Henon map:

$$\nu_x=0.168, \nu_y=0.201$$

Modulation amplitude=1

$$\kappa=1.2^{+0.5}_{-0.5}$$

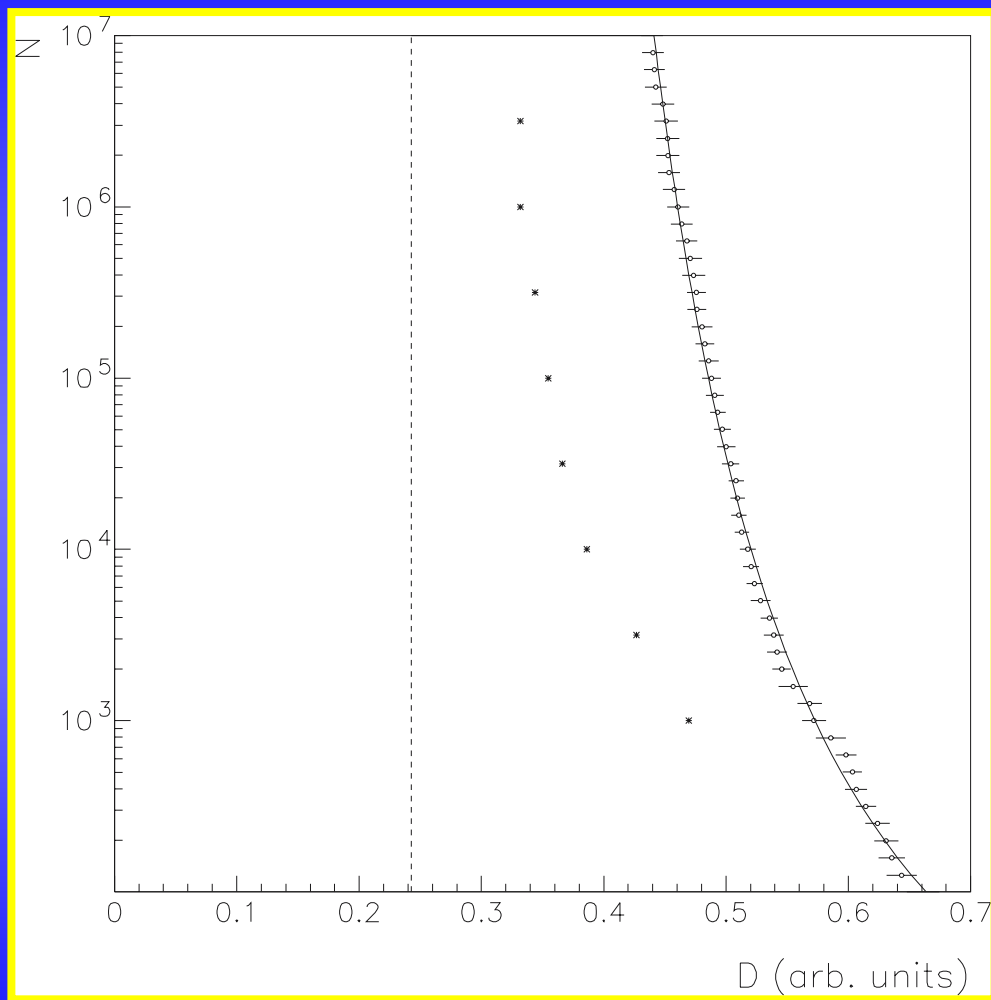
$$A=0.40^{+0.04}_{-0.09}$$

$$B=0.6^{+0.2}_{-0.1}$$

Small stars represent
Lyapunov estimate



Time-dependent effects 4/4



Simulation results for
modulated Henon map:

$$\nu_x=0.168, \nu_y=0.201$$

Modulation amplitude=4

$$\kappa=0.6^{+0.5}_{-0.4}$$

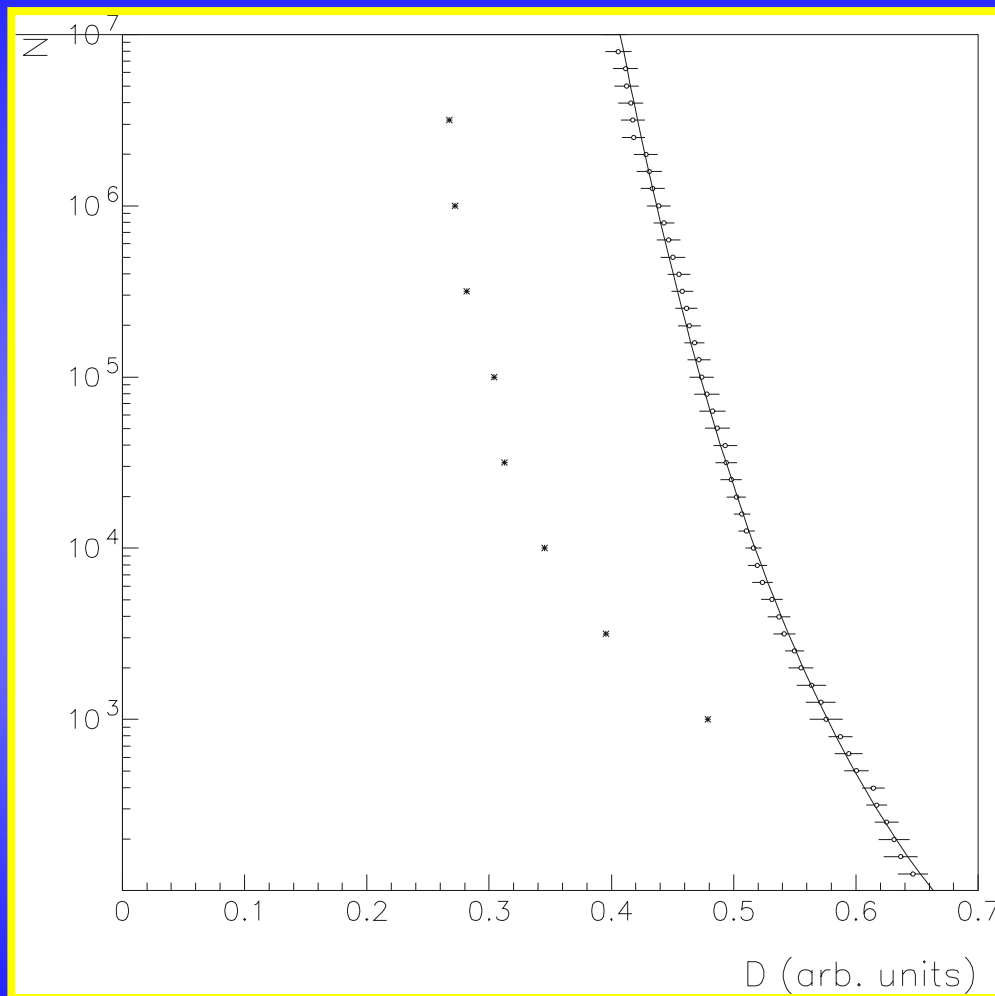
$$A=0.24^{+0.13}_{-0.56}$$

$$B=0.6^{+0.5}_{-0.0}$$

Small stars represent
Lyapunov estimate



Time-dependent effects 4/4



Simulation results for modulated Henon map:

$$v_x=0.168, v_y=0.201$$

Modulation amplitude=16

$$\kappa=0.1^{+0.4}_{-0.5}$$

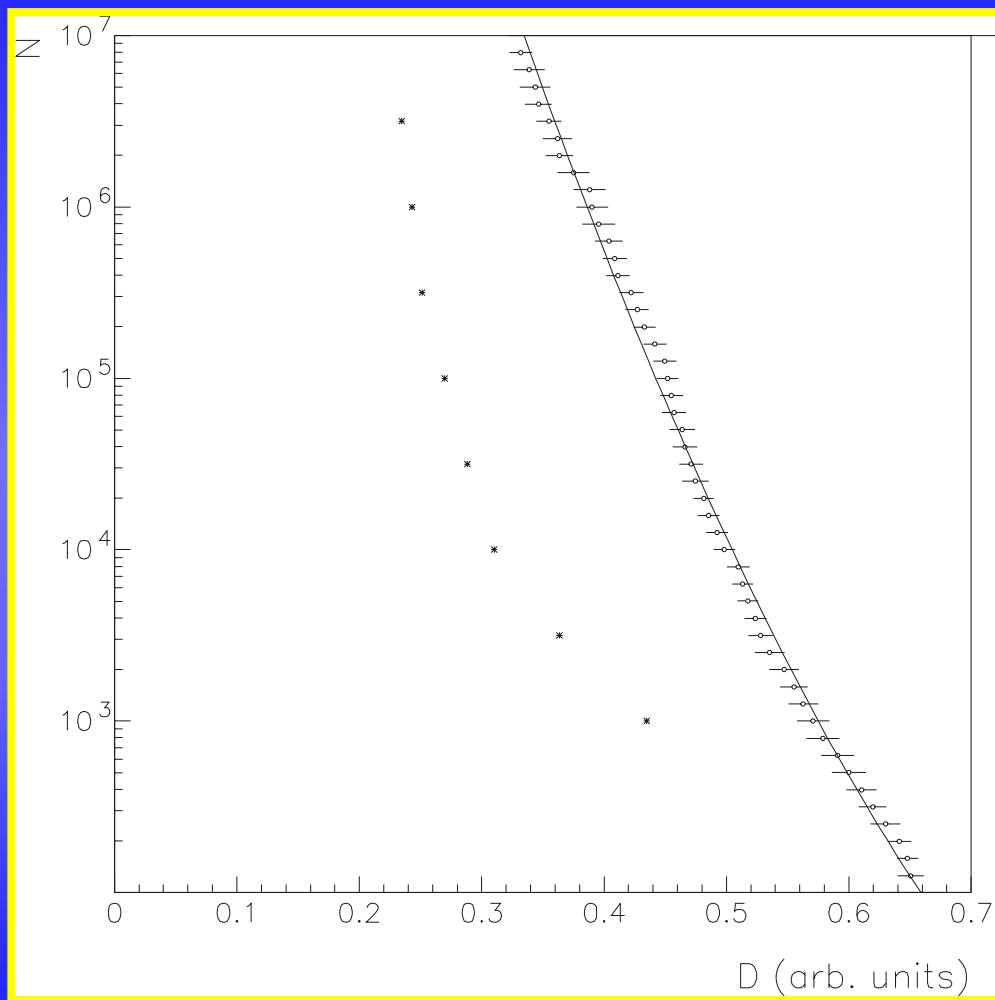
$$A=-1.5$$

$$B=2.3$$

Small stars represent Lyapunov estimate



Time-dependent effects 4/4



Simulation results for
modulated Henon map:

$$v_x=0.168, v_y=0.201$$

Modulation amplitude=64

$$\kappa = -0.5^{+0.4}_{-0.3}$$

$$A = 1.0^{+2.0}_{-0.2}$$

$$B = -0.3^{+0.2}_{-2.0}$$

Small stars represent
Lyapunov estimate